

PRESSURE DROP OF MIST FLOW OF AIR AND
WATER IN A VERTICAL PIPE

By

WILLIAM DEAN LEONARD

//

Bachelor of Science

Oklahoma State University of Agriculture and Applied Science

Stillwater, Oklahoma

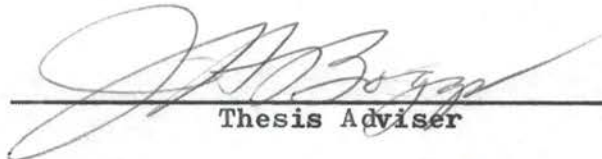
1957

Submitted to the faculty of the Graduate College
of the Oklahoma State University of
Agriculture and Applied Science
in partial fulfillment of the
requirements for the degree
of
MASTER OF SCIENCE
August, 1958

NOV 5 1958

PRESSURE DROP OF MIST FLOW OF AIR AND
WATER IN A VERTICAL PIPE

Thesis Approved:



Thesis Adviser





Dean of the Graduate College

409953

PREFACE

The purpose of this thesis is to determine the pressure drop that occurs in mist flow. Mist flow has been neglected in much of the work that has been done in the field of two-component, two-phase flow. The lack of material concerning mist flow is very apparent in the literature.

In the research carried out in this investigation an expression of the pressure drop of mist flow in terms of the properties of the components has been found. Air and water were used as the components.

This work has been performed through a graduate fellowship sponsored by the Pan American Petroleum Corporation to whom thanks is given for their enthusiasm in this work and the financial assistance awarded.

I thank Dr. J. H. Boggs for his suggestion for carrying out the research and for the writing of this paper. Professor B. S. Davenport who gave needed advice in setting up the equipment certainly deserves a word of thanks. I also thank Professor John W. Hamblen for his help in programming, for solution on an IBM 650 digital computer, the necessary computations.

To my father, Professor C. M. Leonard who throughout this work has given guidance and understanding, I dedicate this paper.

TABLE OF CONTENTS

Chapter	Page
I. INTRODUCTION	1
II. REVIEW OF THE LITERATURE	3
III. THE RESEARCH EQUIPMENT	12
IV. PROCEDURE	18
V. THE DATA	21
VI. CORRELATING THE DATA	27
VII. COMPUTATIONS	37
VIII. CONCLUSIONS	41
BIBLIOGRAPHY	43
APPENDIX	45

LIST OF TABLES

Table	Page
I. DATA FOR MIST FLOW	23
II. DATA FOR AIR ONLY	26
III. CORRELATION ERROR	35
IV. CORRELATION PARAMETERS	39

LIST OF ILLUSTRATIONS

Figure	Page
1. Flow patterns of vertical, two-component, two-phase flow	5
2. Martinelli correlation for viscous-turbulent flow . . .	7
3. Relation of liquid-volume fraction to \bar{X}	9
4. Pressure tap detail	12
5. Mixing section	14
6. Flow diagram	17
7. Calibration curves of water rotameters	20
8. Pressure drop for the gas flowing alone	22
9. Nesbit's flow pattern chart	28
10. Relation of ϕ_{mist} to X_{mist}	30
11. Relation between $\phi_{mist}^{0.293}$ and $X_{mist}^{0.257}$	32

SYMBOLS AND ABBREVIATIONS

A	cross-sectional area, sq ft
C_1	experimental constant
C_g	experimental constant
cfm	cubic feet per minute
cfs	cubic feet per second
cu ft	cubic foot(feet)
d	inside diameter, ft
Eq.	equation(s)
$^{\circ}$ F	degrees Fahrenheit
Fig.	figure
ft	foot(feet)
g	acceleration of gravity, ft per sec-sec
\bar{G}	mass rate of flow, lbs per sq ft-sec
hr	hour
in.	inch(es)
in. hg abs	inches of mercury absolute
lbs	pound(s)
min	minute
mm	millimeter
No. or no.	number
P	absolute pressure, psf
P_{avg}	average static pressure, psf

psf	pounds per square foot
psi	pounds per square inch
psig	pounds per square inch gage
ΔP	pressure drop, psf
$\left[\frac{\Delta P}{\Delta L}\right]_g$	pressure drop of gas flowing alone, psi per ft
$\left[\frac{\Delta P}{\Delta L}\right]_{mist}$	pressure drop of mist flow, psi per ft
$\left[\frac{\Delta P}{\Delta L}\right]_{tp}$	pressure drop of two-component, two-phase flow, psi per ft
R	gas constant, ft per $^{\circ}$ R
$^{\circ}$ R	degrees Rankine
Re_g	Reynolds number of gas flowing alone
R_l	liquid-volume fraction, percent
sec	second
sq ft	square foot(feet)
T	absolute temperature, $^{\circ}$ R
U_l	pseudo liquid velocity, ft per sec
U_g	pseudo gas velocity, ft per sec
\bar{U}_l	average velocity of liquid, ft per sec
V_l	liquid volume rate, cfs
V_g	gas volume rate, cfs
W_l	liquid rate, lbs per min
W_g	gas rate, lbs per min
X_{mist}	a dimensionless parameter of mist flow
X_{tt}	a dimensionless parameter of turbulent-turbulent flow
X_{vt}	a dimensionless parameter of viscous-turbulent flow
X_{tv}	a dimensionless parameter of turbulent-viscous flow

X_{vv}	a dimensionless parameter of viscous-viscous flow
\bar{X}	a dimensionless parameter of two-component, two-phase flow
μ_l	liquid viscosity, lbs per sec-ft
μ_g	gas viscosity, lbs per sec-ft
ρ_l	liquid density, lbs per cu ft
ρ_g	gas density, lbs per cu ft
ρ_{gl}	average density of the mixture, lbs per cu ft
ϕ_g	a dimensionless parameter of two-component, two-phase flow
ϕ_{mist}	a dimensionless parameter of mist flow

CHAPTER I

INTRODUCTION

One of the present day methods of oil recovery uses air as a drilling fluid. Being able to predict the pressure drop that occurs as water is picked up and carried to the surface in this air stream is important. Also, the pressure drop that occurs in pipe lines carrying two different fluids is of interest.

Thus, as a research project undertaken for Pan American Petroleum Corporation, a method of predicting the pressure drop that occurs in the type of two-component, two-phase flow known as mist flow has been devised. The particular mist flow that this investigation was interested was vertically upward, isothermal mist flow.

The study of two-component, two-phase flow has been a problem which has yielded little to analytical solution. The work which has been done in evaluating pressure drop and heat transfer is largely of an experimental nature. Several investigators have made studies of this type of flow in an effort to determine an expression that would predict, with a good degree of accuracy, the pressure drop which occurs during two-component, two-phase flow.

Various flow patterns can exist in two-component, two-phase flow and one school of thought is to correlate the pressure drop specifically as it occurs during each of the flow patterns.

Another plan is to correlate the pressure drop for two-component, two-phase flow ignoring the flow pattern that exists.

To determine the relationship that exists between the variables of mist flow (density, pressure, viscosity, etc.), the necessary equipment was set up in the Mechanical Engineering Laboratory of Oklahoma State University. From the data accumulated, a correlation was obtained that would predict the pressure drop for mist flow.

CHAPTER II

REVIEW OF THE LITERATURE

An analysis of two-component, two-phase flow is complicated by the type of flow pattern; whether the flow is horizontal, vertical upward, vertical downward, or at some other angle; and whether the components are in viscous or turbulent flow conditions.

Mist flow during vertical upward flow is a special type of flow pattern which can exist during two-component, two-phase flow. It has been found that as a gas is pumped into a line which is delivering a liquid isothermally and vertically upward, a type of flow exists called bubble flow. In general the paths of the bubbles are helices. As the air rate is increased the bubbles form slugs which occupy the entire cross-section of the channel and move upward with the same velocity as that of the liquid. This type of flow is called slug flow. A further increase in the air rate causes the slugs of water to separate allowing the slugs of air to connect. The liquid then occupies an annular path around the channel and the interface between the liquid and gas is rough and uneven. This flow pattern is known as semi-annular. Annular flow is obtained by additional increase of the gas rate which causes the gas core to become clearly defined. At very high gas rates the liquid breaks up into fine droplets and

is dispersed evenly into the entire flow area. This is called mist flow. These flow patterns are shown in Fig. 1.

Several methods have been used to analyze the pressure drop that occurs in two-component, two-phase flow. One of the most encouraging schemes is set forth by Martinelli (9). However, his experiments did not include data for mist flow. In Martinelli's work he describes the flow by stating whether each component is flowing viscously or turbulently. This is known as the flow mechanism. Note that this method makes no distinction as to the type of flow occurring such as mist, slug, etc. A Reynolds number of 2000 is used to divide viscous flow from turbulent flow.

Martinelli states that:

$$\left[\frac{\Delta P}{\Delta L} \right]_{tp} = \phi_g^2 \left[\frac{\Delta P}{\Delta L} \right]_g \quad (1)$$

where $\left[\frac{\Delta P}{\Delta L} \right]_{tp}$ = pressure drop for two-component, two-phase flow, psi per ft;

$\left[\frac{\Delta P}{\Delta L} \right]_g$ = pressure drop for the gas flowing alone, psi per ft; and

ϕ_g = a dimensionless parameter.

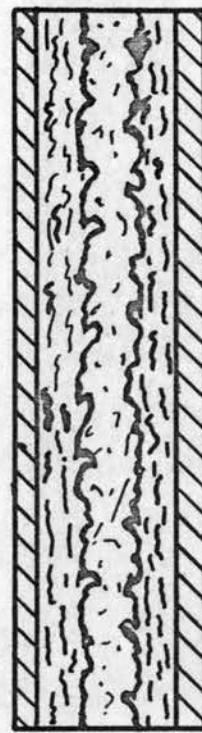
The dimensionless parameter, ϕ_g , is a function of another dimensionless variable, X. The variable X is a function of the ratios of weight rates, densities, and viscosities of the liquid and gas; the Reynolds number; and whether each component is flowing viscously or turbulently. The relation between ϕ_g and X for the case of the gas flowing turbulently and the liquid flow-



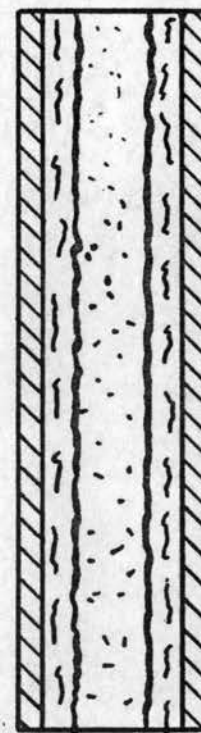
Bubble flow



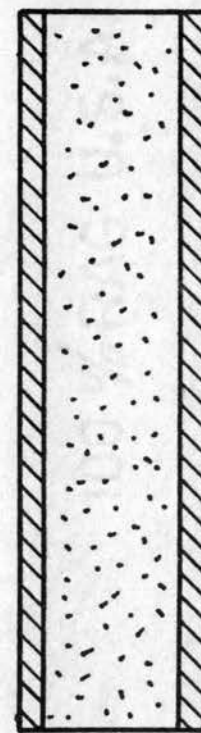
Slug flow



Semi-annular flow



Annular flow



Mist flow

Fig. 1. Flow patterns of vertical, two-component, two-phase flow

ing viscously is shown in Fig. 2. According to this figure, ϕ_g does not exist below a value of two. Thus, according to Eq. 1 the smallest pressure drop that could occur in this type of flow is four times the pressure drop of the gas flowing alone.

The following notation is used to denote the particular flow mechanism that exists:

X_{tt} - liquid turbulent, gas turbulent;

X_{vt} - liquid viscous, gas turbulent;

X_{tv} - liquid turbulent, gas viscous;

X_{vv} - liquid viscous, gas viscous.

The Reynolds number of each component of the flow is calculated using the total flow area through which the mixture is flowing. This results in a pseudo Reynolds number which is used throughout this investigation. For mist flow the gas rates are very high and the water rates are relatively low. Therefore, the type of flow mechanism that is usually encountered in mist flow can be described as viscous-turbulent. For viscous-turbulent flow:

$$X_{vt} = Re_g^{-0.8} \frac{C_1}{C_g} \frac{W_1}{W_g} \frac{\rho_g}{\rho_1} \frac{\mu_1}{\mu_g} \quad (2)$$

where Re_g = Reynolds number for the gas flowing alone;

C_1 = 64 for smooth pipes;

C_g = 0.184 for smooth pipes;

W_1 = liquid rate, lbs per min;

W_g = gas rate, lbs per min;

ρ_1 = liquid density, lbs per cu ft;

ρ_g = gas density, lbs per cu ft;

μ_1 = liquid viscosity, lbs per sec-ft; and

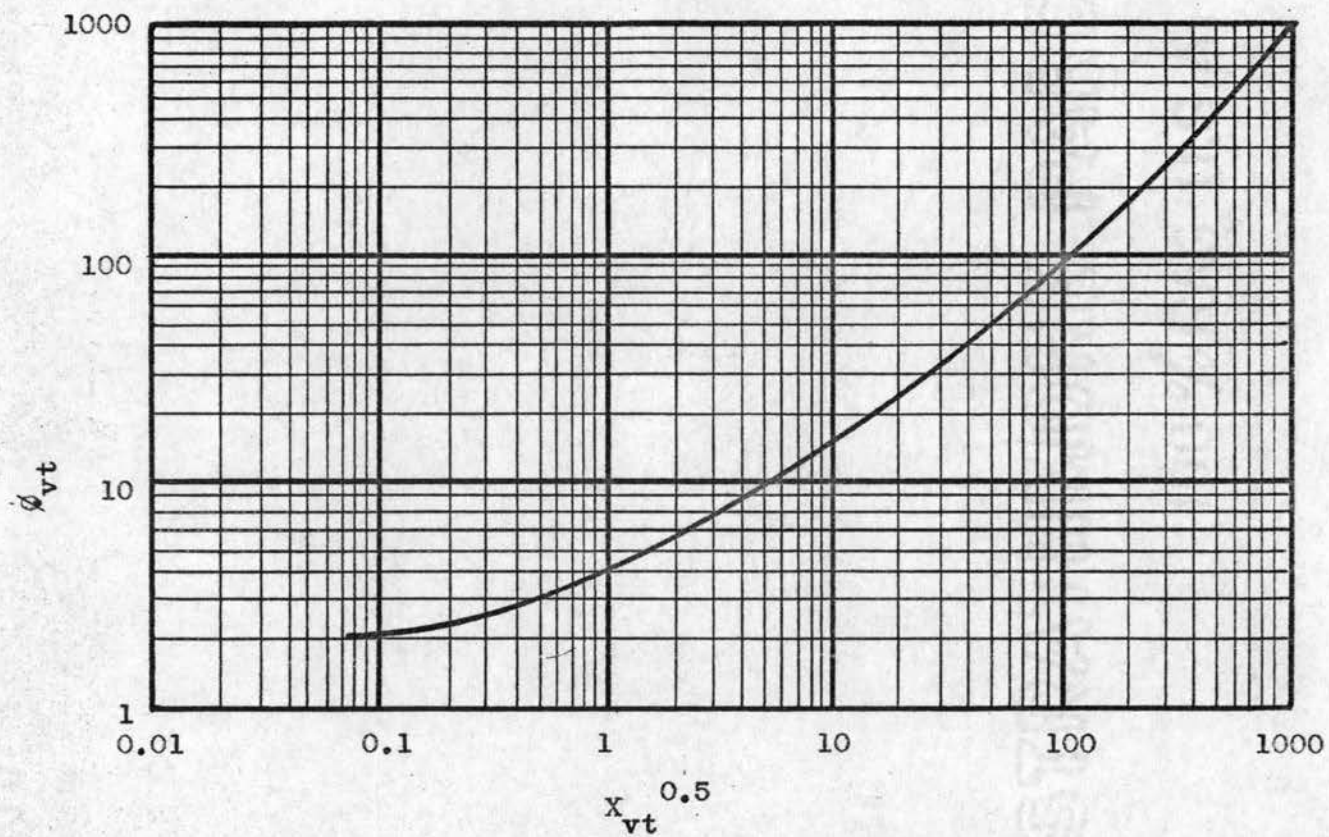


Fig. 2. Martinelli correlation for viscous-turbulent flow

μ_g = gas viscosity, lbs per sec-ft.

Using Eq. 1 and 2 makes it possible to predict the pressure drop of two-component, two-phase flow knowing only readily obtainable information.

Later Martinelli and Lockhart (7) correlated all types of flow into one correlation. Thus the former X was replaced by a new parameter, \bar{X} . The relations that exist between X and \bar{X} are:

$$X_{tt} = \bar{X}_{tt}^{1.11} \quad (3)$$

$$X_{vt} = \bar{X}_{vt}^2 \quad (4)$$

$$X_{tv} = \bar{X}_{tv}^2 \quad (5)$$

$$X_{vv} = \bar{X}_{vv}^2 \quad (6)$$

An extension of Martinelli's and Lockhart's work showed that the liquid-volume fraction was a function of the parameter, \bar{X} . The liquid-volume fraction is defined as the percent of the flow volume occupied by the liquid. Thomsen (12) and Taylor (11) measured the liquid-volume fraction, R_1 , by trapping a representative sample of the flow mixture between quick-closing valves, blowing down the pipe, and measuring the liquid content. Lockhart, however, measured R_1 by trapping the liquid between quick-closing valves, washing out the tube with a large quantity of volatile solvent, and evaporating the excess solvent. Both of these experiments confirmed that the liquid-volume fraction could be expressed as a function of \bar{X} . A plot of this relation is shown in Fig. 3.

The postulates upon which Lockhart and Martinelli based their calculations are:

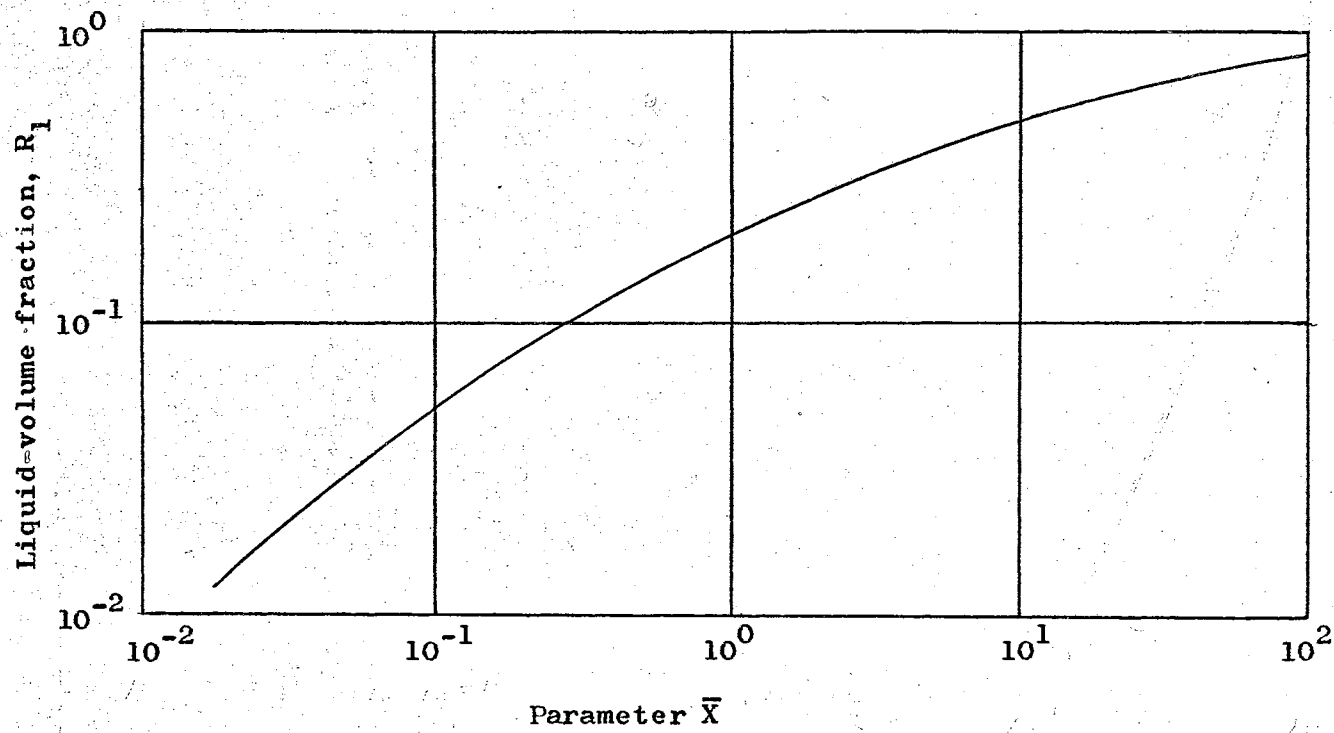


Fig. 3 Relation of liquid-volume fraction to \bar{X}

1. Static pressure drop for the liquid component must equal the static pressure drop for the gaseous component regardless of the flow pattern as long as an appreciable radial static pressure difference does not exist.
2. The volume occupied by the liquid plus the volume occupied by the gas at any instant must equal the total volume of the pipe.

Taylor's and Thomsen's experiments were carried out using air as the gas; and water, kerosene, diesel fuel, SAE 40 oil, or benzene as the liquid.

Yagi and Sasaki (14) investigated vertical mist flow using glass tubes of 8, 10.25, 12.5, and 17.5 mm inside diameter. They used air and various liquids. As a result of their experiments, Yagi and Sasaki concluded that:

$$\left[\frac{\Delta P}{\Delta L} \right]_{\text{mist}} = 5000 \rho_{gl} \left[\frac{\bar{U}_1^2}{2gd} \right]^{0.75} \left[\frac{\bar{G}d}{\mu_1} \right]^{-0.6} \quad (7)$$

where $\left[\frac{\Delta P}{\Delta L} \right]_{\text{mist}}$ = pressure drop for mist flow, psi per ft;
 ρ_{gl} = average density of the mixture, lbs per cu ft;
 \bar{U}_1 = average velocity of the liquid, ft per sec;
 d = inside diameter of tube, ft;
 \bar{G} = mass rate of flow of the mixture, lbs per sq ft-sec;
 μ_1 = viscosity of the liquid, lbs per sec-ft; and
 g = acceleration of gravity, ft per sec-sec.

Several investigators have attempted to correlate the pressure drop in mist flow by assuming the gas-liquid mixture to be a

homogeneous substance. However, the determination of the properties of the new substance is difficult to attain. How such items as viscosity should be evaluated make this method unpopular.

Yagi and Kato (13) stated that the pressure drop in horizontal mist flow could be expressed as:

$$\left[\frac{\Delta P}{\Delta L} \right]_{\text{mist}} = \left[\frac{\Delta P}{\Delta L} \right]_g \left(1.5 + 0.83 \frac{\mu_1}{d} \right) \left(1 + \frac{U_1}{U_g} \frac{P_{\text{avg}}}{P_i} \right) \left(1 + \frac{V_1}{V_g} \right)^{0.8} \frac{P_i}{P_{\text{avg}}} \quad (8)$$

where $\left[\frac{\Delta P}{\Delta L} \right]_{\text{mist}}$ = pressure drop for mist flow, psi per ft;

$\left[\frac{\Delta P}{\Delta L} \right]_g$ = pressure drop for gas flowing alone, psi per ft;

μ_1 = liquid viscosity, lbs per ft-sec;

d = inside diameter of tube, ft;

U_1 = pseudo liquid velocity, ft per sec;

U_g = pseudo gas velocity, ft per sec;

P_{avg} = average static pressure of mixture, psf;

P_i = inlet static pressure of mixture, psf;

V_1 = liquid volume rate, cfs; and

V_g = gas volume rate, cfs.

In work done by Bergelin (2) he states that the orientation of the tube has little effect upon the pressure drop during two-component, two-phase flow at high gas rates.

CHAPTER III

THE RESEARCH EQUIPMENT

Pyrex tubing, 12 ft long and with an inside diameter of 0.301 in. and an outside diameter of 0.500 in. was used as a test section. Pressure taps were located 10 ft apart thus giving 40 pipe diameters of undisturbed flow both before and after reaching the respective pressure tap. The taps were made by drilling $3/32$ in. holes perpendicular to the wall of the test section with brass rod and emery powder-oil solution. Then short glass capillary tubes were shaped to fit the test section and then ground to give a snug fit as shown in Fig. 4. They were held in place with cement. The test section was then mounted

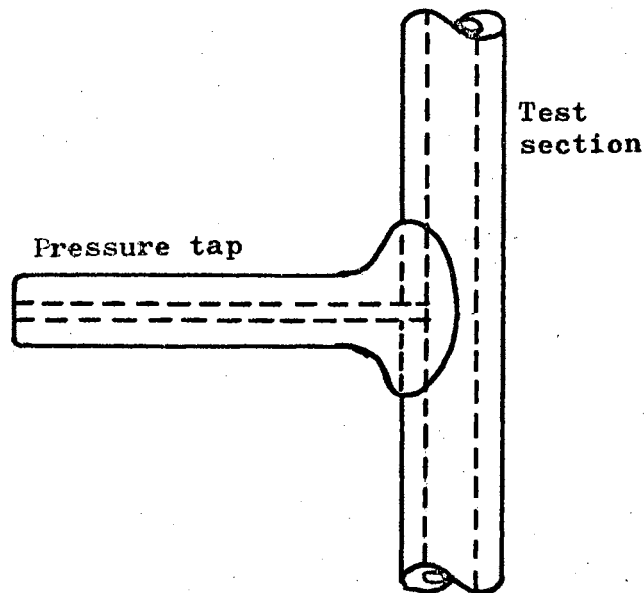


Fig. 4. Pressure tap detail

in a vertical position with the entrance at the lower end.

The mixing section was made from 2 in. copper pipe shaped to the cross-section shown in Fig. 5. Four $2\frac{1}{64}$ in. holes were drilled into each side of this shell and steel nuts were tapped to $\frac{1}{8}$ in. taper pipe threads. These were then soldered over each hole. A screening section was made from 1 in. copper pipe 2 in. in length and 160 mesh brass screenwire. This unit was soldered to the top of the mixing section to insure that the water entered the test section in the form of a mist. To the top of the screening section a reduction to $\frac{1}{2}$ in. copper tubing was brazed. Into the bottom of the mixing section was soldered a $1\frac{1}{4}$ in. copper pipe 6 in. long to which the air line was attached. Also in the bottom of the mixing section a drain valve was provided.

Eight nozzles were designed to spray the water into the mixing section. These screwed into the nuts provided on the sides of the mixing section. The nozzles were made by soldering a plate of 30 gauge brass shim stock over the hole in a $\frac{1}{4}$ in. flare to $\frac{1}{8}$ in. pipe brass fitting. Into the center of the brass plate a #80 hole was drilled. The necessary water manifolds were built from 1 in. and $\frac{1}{4}$ in. copper tubing and were connected to the mixing section with valves to control the flow of water to each nozzle as shown in Fig. 5. This completed the construction of the mixing section. The mixing section was then mounted in place and connected to the lower end of the test section by a 3 in. length of rubber tubing.

Rotameters were used to measure both the rate of air and water flow. Air velocities in the range of 70 to 200 ft per sec

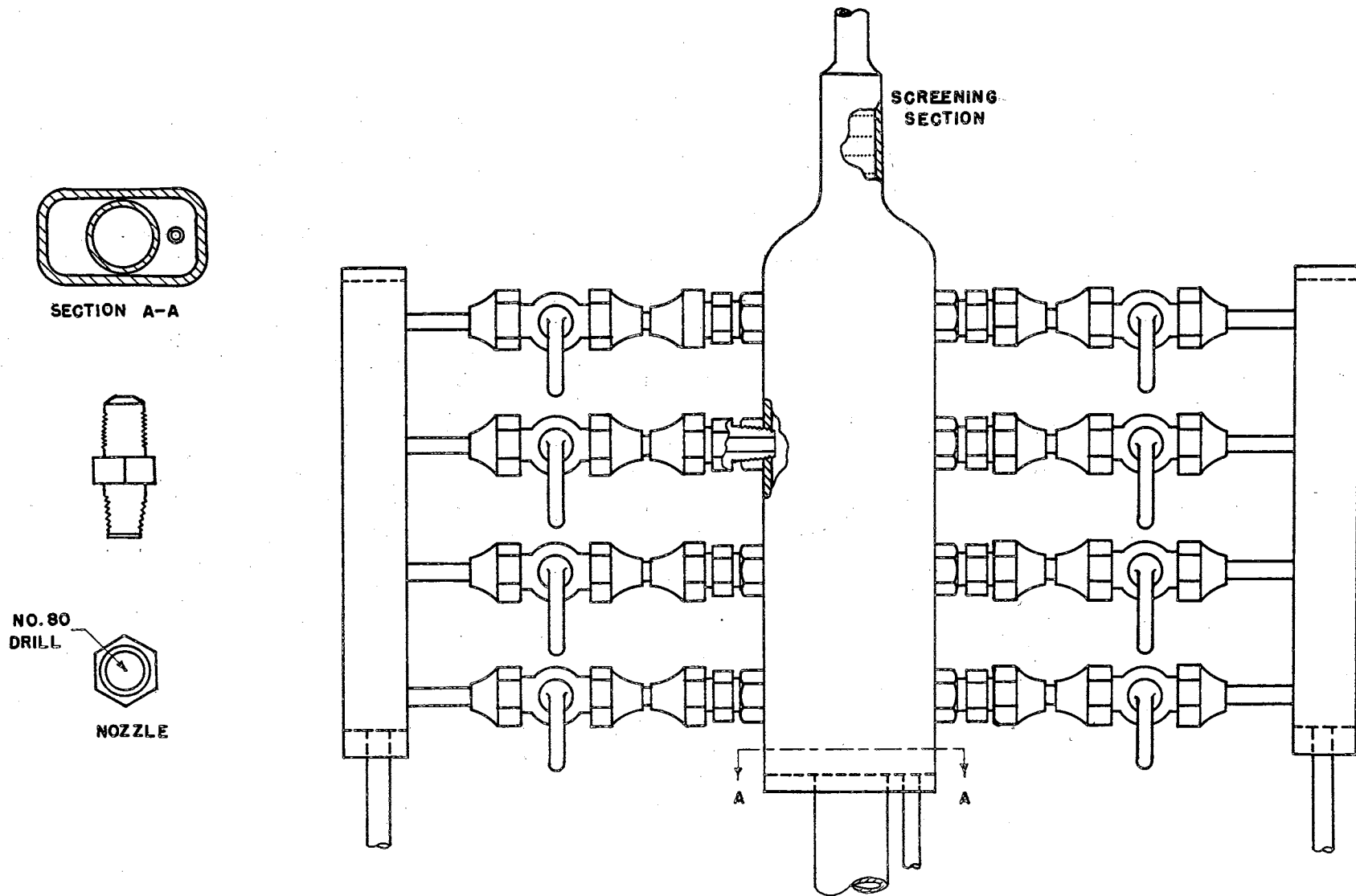


Fig. 5. Mixing section

were desired. Thus a rotameter with a range up to 8 cfm was used to measure the air rate. It had $3/4$ in. pipe entrance and exit fittings and $3/4$ in. galvanized pipe was used to connect the exit to the entrance of the mixing section. A $3/4$ in. globe valve was used to control the flow of air to the rotameter. Both a temperature well and a pressure tap were provided so that the air temperature and pressure as the air entered the rotameter could be measured.

Water rates in the range of 0 to 0.5 lbs per min were used. To measure these rates, two rotameters were used. One had a range of 50 to 130 lbs per hr of liquid of a specific gravity of 0.80 and the second one had a range of 20 to 60 lbs per hr of liquid of the same specific gravity. In order to obtain a complete range of water rates the small rotameter was used to measure the difference between the water supplied by the large rotameter and the water which was supplied to the mixing section. Thus a range of water rates was available from 0 to 2.2 lbs of water per min using these rotameters. A centrifugal pump was used to maintain a head of approximately 70 psig on the water system. The water was delivered by $3/8$ in. copper tubing from the rotameters to the mixing section. A 36 in. mercury manometer was used to measure the pressure drop in the test section. The test section was connected to the manometers with air filled rubber tubing. A 36 in. mercury manometer was also used to measure the static pressure at the entrance to the test section.

The air was supplied by a double-acting, two-cylinder compressor. The air was delivered into storage tanks and was then

delivered to a pressure regulator which maintained a maximum pressure of 30 psig on the system. From the regulator the air was passed through a filter which consisted of a steel tank with cotton batting to absorb any moisture or oil that might be entrained in the air.

The top of the test section was connected to a 3/8 in. globe valve with rubber tubing and then exhausted to the atmosphere. This made it possible to vary the average pressure in the test section.

Figure 6 shows the complete flow diagram of the equipment.

The appendix gives manufacturers of the equipment.

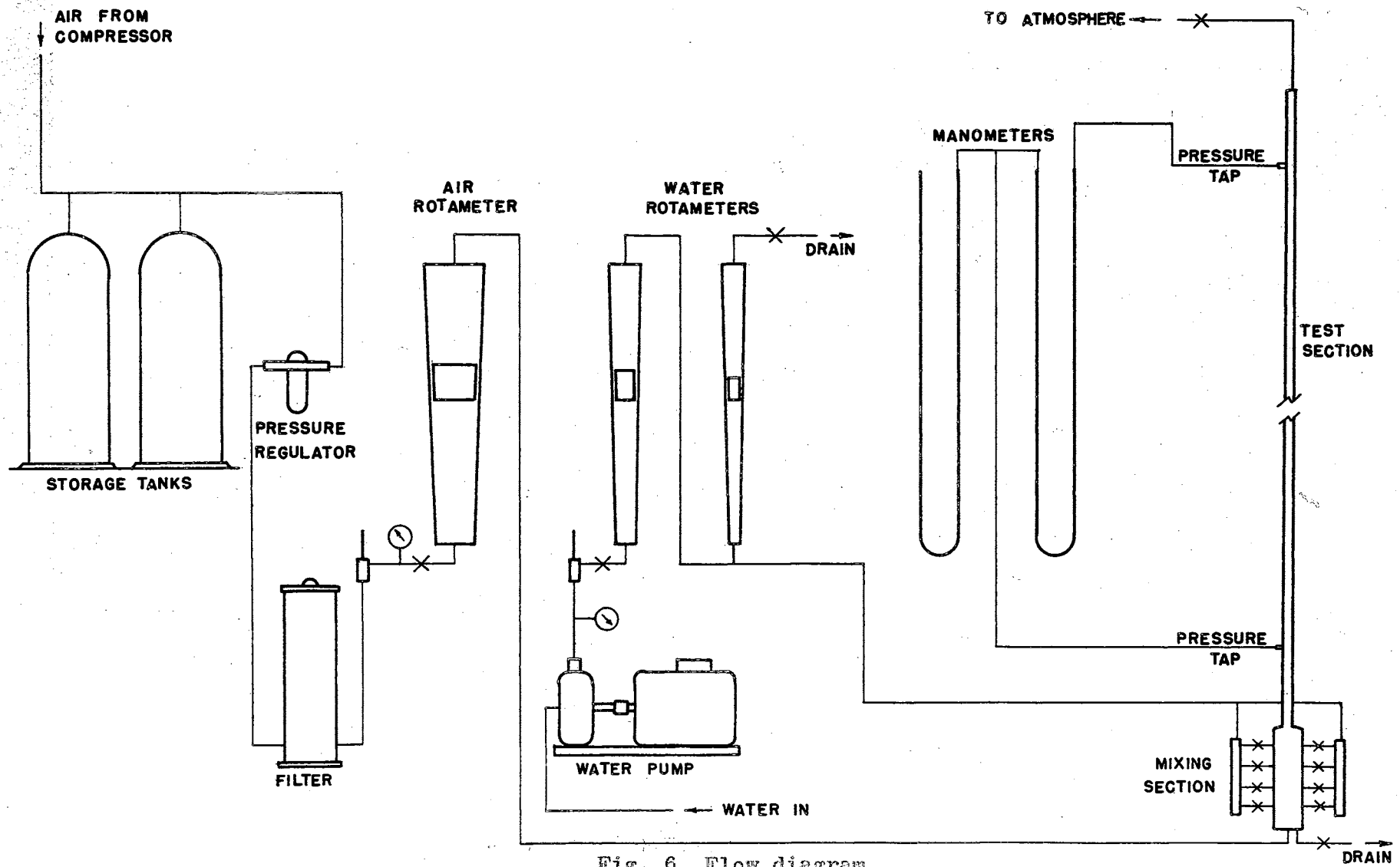


Fig. 6. Flow diagram

CHAPTER IV

PROCEDURE

The procedure for obtaining data was begun by starting the compressor and opening the main water valve. Air was allowed to flow through the test section and water into the mixing section and out of the drain. During the time when the water and air systems reached equilibrium, ambient temperature and pressure were noted. Water and air temperatures were then recorded.

The air rotameter was then adjusted to a desired air rate and kept at this position as the water rate was varied to the desired rates. Air rates used ranged from 4 cfm to 8 cfm. Air rates lower than 4 cfm allowed some water to flow annularly up the test section. Water rates were varied from 0 to 1.3 lbs per min. Larger water rates than this also caused annular flow.

After equilibrium was reached at each air and water rate, the pressure drop in the test section and the static pressure at the entrance to the test section were noted. The existing conditions made it possible to have the air and water enter the test section within $\pm 1^{\circ}$ F of the ambient temperature. This condition made it unnecessary to use any insulation on the test section.

At the conclusion of a series of runs the ambient temperature and pressure as well as the temperature of the air and water were again recorded.

The calibration of the water rotameters had been carried out previously. The calibration curves of these rotameters are shown in Fig. 7.

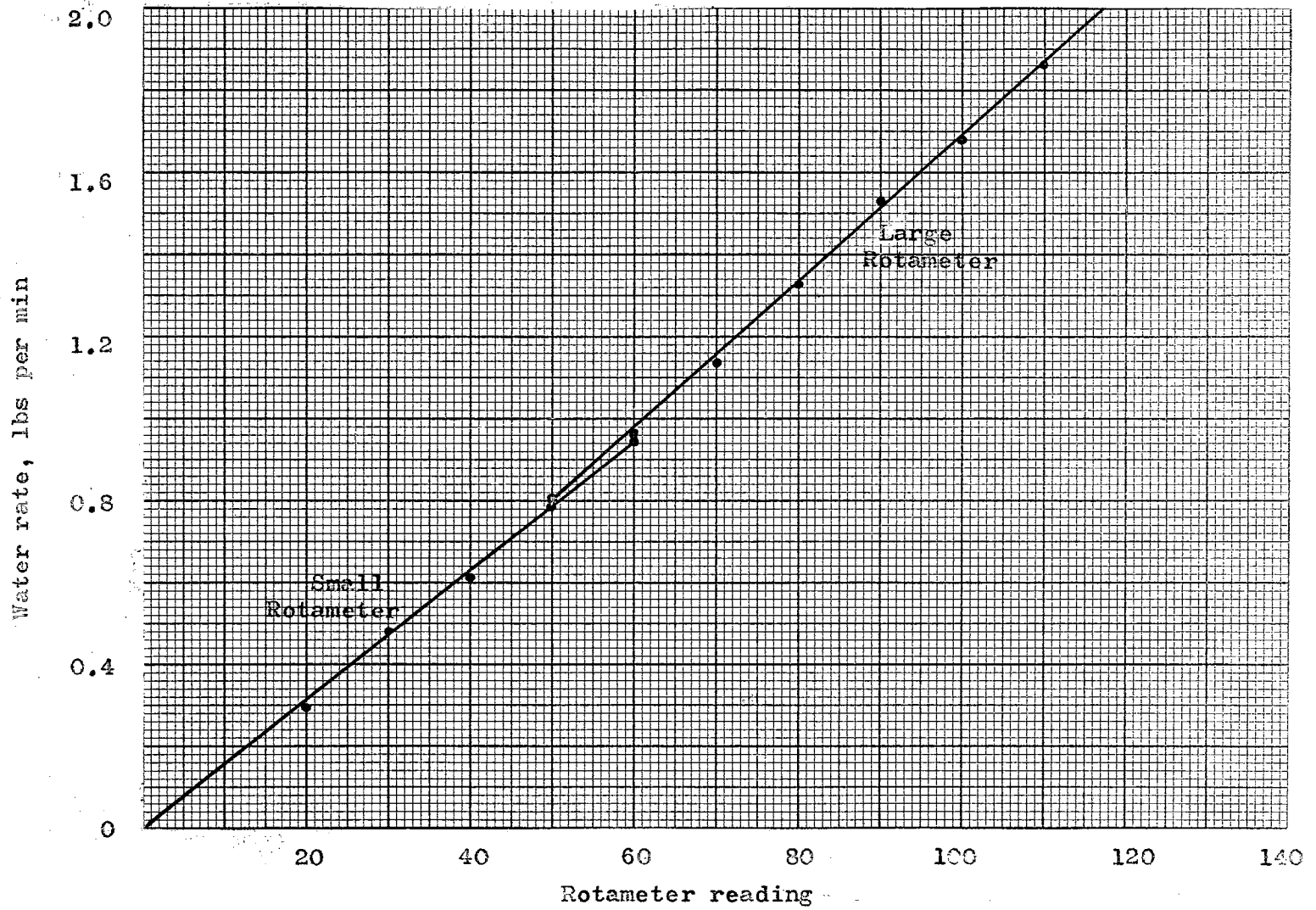


Fig. 7. Calibration curves of water rotameters

CHAPTER V

THE DATA

A digital computer was used to make the calculations from the five items of data which were secured for each run. The five items recorded were: (1) run number; (2) air rate; (3) water rate; (4) average static pressure, $(2 P_i + \Delta P)/2$; and (5) the pressure drop of the mixture. These data are shown in Table I.

There were 45 runs made with air alone at various average static pressures which supplied the pressure drop of the gas flowing alone and the information for computing Re_g . These data are shown in Table II. The plot of the average static pressure versus the pressure drop for the gas flowing alone is shown in Fig. 8.

All data are taken at 65° F.

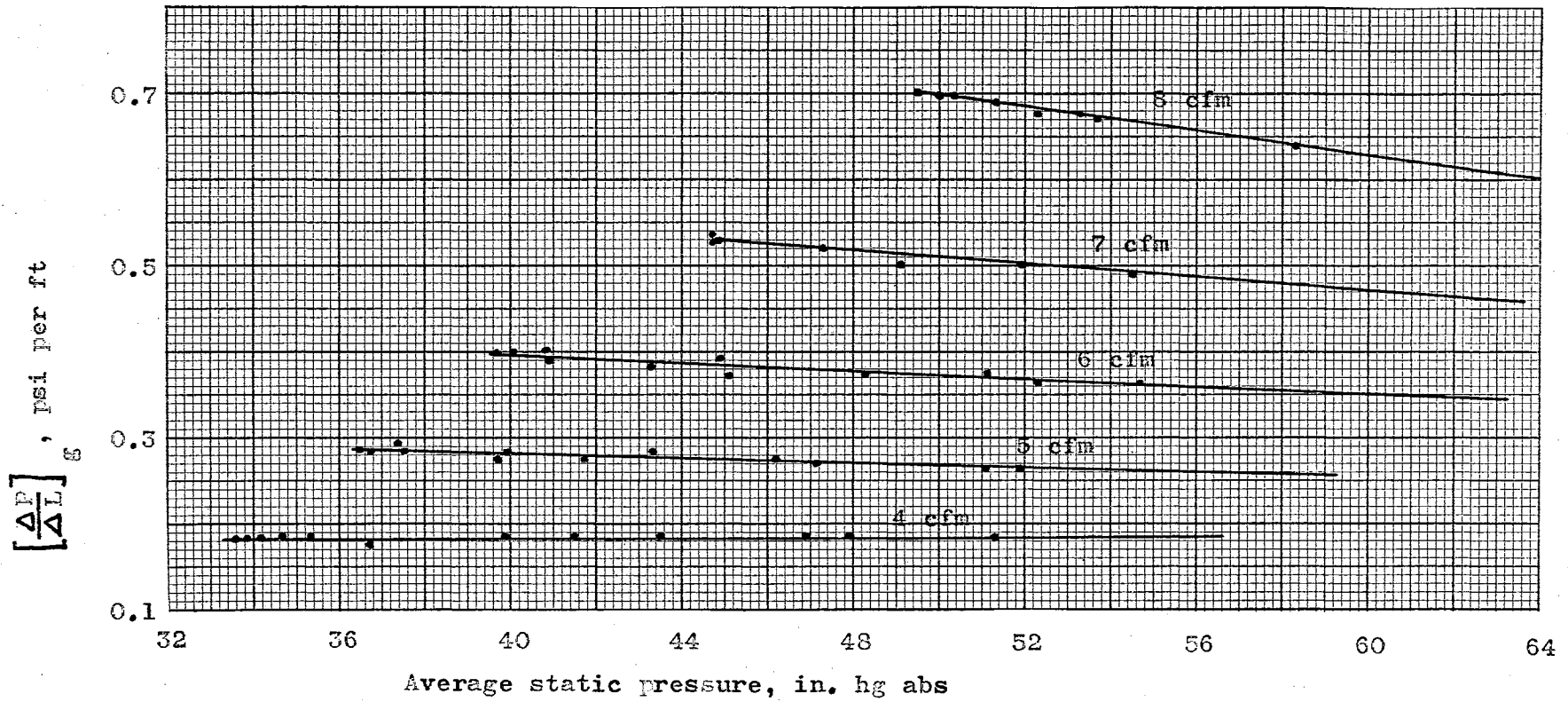


Fig. 8. Pressure drop for the gas flowing alone

TABLE I
DATA FOR MIST FLOW

Run No.	Air rate; cfm	Water rate; lbs per min	Pressure drop, mixture; psi per ft	Pressure drop, gas; psi per ft	Average static pressure; in. hg abs
1	4	0.062	0.314	0.185	37.22
2	4	0.095	0.334	0.185	39.02
3	4	0.128	0.402	0.185	39.62
4	4	0.160	0.441	0.185	40.62
5	4	0.190	0.451	0.185	40.82
6	4	0.221	0.460	0.185	41.22
7	4	0.254	0.470	0.185	41.22
8	4	0.286	0.500	0.185	41.62
9	4	0.318	0.540	0.185	42.62
10	4	0.000	0.187	0.187	33.89
11	4	0.318	0.530	0.185	41.89
12	4	0.349	0.550	0.185	42.69
13	4	0.380	0.564	0.185	43.89
14	4	0.413	0.608	0.185	44.89
15	4	0.444	0.608	0.185	44.89
16	4	0.477	0.628	0.185	45.69
17	4	0.507	0.705	0.185	47.49
18	4	0.540	0.745	0.185	48.69
19	4	0.570	0.774	0.185	49.69
20	4	0.602	0.765	0.185	50.09
21	4	0.634	0.804	0.185	50.69
22	5	0.000	0.284	0.284	36.69
23	5	0.318	0.774	0.270	49.49
24	5	0.349	0.795	0.270	50.49
25	5	0.380	0.804	0.268	50.89
26	5	0.413	0.833	0.266	51.49
27	5	0.444	0.882	0.266	52.49
28	5	0.477	0.924	0.265	54.49
29	5	0.507	0.944	0.263	54.89
30	5	0.540	0.982	0.261	55.69
31	5	0.570	1.000	0.260	56.09
32	5	0.602	1.010	0.258	56.49
33	5	0.634	1.090	0.256	58.49
34	5	0.667	1.100	0.255	58.89
35	5	0.000	0.295	0.295	37.41
36	5	0.031	0.460	0.283	40.81
37	5	0.062	0.440	0.280	40.81
38	5	0.095	0.480	0.278	41.41
39	5	0.128	0.510	0.276	41.61
40	5	0.160	0.598	0.275	43.41
41	5	0.190	0.579	0.274	44.81
42	5	0.221	0.619	0.273	46.01
43	5	0.254	0.680	0.272	48.01

TABLE I (Continued)

Run No.	Air rate; cfm	Water rate; lbs per min	Pressure drop, mixture; psi per ft	Pressure drop, gas; psi per ft	Average static pressure; in. hg abs
44	5	0.286	0.707	0.271	49.21
45	5	0.318	0.735	0.270	50.01
46	5	0.000	0.284	0.284	39.88
47	5	0.031	0.314	0.278	41.88
48	5	0.062	0.372	0.275	42.68
49	5	0.095	0.402	0.275	42.88
50	5	0.128	0.549	0.273	47.08
51	5	0.160	0.588	0.271	48.48
52	5	0.190	0.600	0.271	49.08
53	5	0.221	0.648	0.270	50.68
54	5	0.254	0.688	0.266	51.08
55	5	0.286	0.707	0.265	53.08
56	5	0.318	0.725	0.265	53.48
57	6	0.000	0.402	0.402	40.78
58	6	0.031	0.450	0.385	41.98
59	6	0.062	0.510	0.382	43.58
60	6	0.095	0.688	0.375	48.38
61	6	0.128	0.735	0.371	49.18
62	6	0.160	0.745	0.371	49.38
63	6	0.190	0.874	0.365	53.18
64	6	0.221	0.882	0.364	53.78
65	6	0.254	0.904	0.363	54.38
66	6	0.286	0.924	0.360	54.78
67	6	0.318	1.020	0.356	57.98
68	6	0.000	0.402	0.402	40.09
69	6	0.318	0.963	0.360	55.89
70	6	0.349	0.963	0.360	56.09
71	6	0.380	1.030	0.356	57.89
72	6	0.413	1.040	0.355	58.29
73	6	0.444	1.080	0.352	60.09
74	6	0.477	1.140	0.350	61.49
75	6	0.000	0.392	0.392	44.88
76	6	0.031	0.431	0.376	46.08
77	6	0.062	0.491	0.374	47.28
78	6	0.095	0.579	0.370	50.28
79	6	0.128	0.707	0.364	54.08
80	6	0.160	0.707	0.362	55.08
81	6	0.190	0.774	0.360	56.08
82	6	0.221	0.833	0.357	58.48
83	7	0.000	0.530	0.530	44.78
84	7	0.031	0.717	0.508	49.58
85	7	0.062	0.755	0.507	50.78
86	7	0.095	0.784	0.502	51.38
87	7	0.128	0.874	0.492	53.98
88	7	0.160	1.000	0.475	57.78

TABLE I (Continued)

Run No.	Air rate; cfm	Water rate; lbs per min	Pressure drop, mixture; psi per ft	Pressure drop, gas; psi per ft	Average static pressure; in. hg abs
89	7	0.190	1.060	0.468	59.98
90	7	0.221	1.090	0.468	60.38
91	7	0.254	1.120	0.460	61.78
92	7	0.286	1.160	0.458	62.98
93	7	0.318	1.170	0.451	63.38
94	7	0.000	0.540	0.540	44.69
95	7	0.318	1.170	0.460	62.49
96	8	0.000	0.697	0.697	49.98
97	8	0.031	0.924	0.658	56.38
98	8	0.062	1.030	0.635	59.78
99	8	0.095	1.050	0.635	59.98
100	8	0.128	1.090	0.620	60.98
101	8	0.160	1.150	0.602	62.98
102	8	0.190	1.180	0.598	63.98

TABLE II

DATA FOR AIR ONLY

Run No.	Air rate, cfm	Pressure drop, psi per ft	Average static pressure, in. hg abs
103	3	0.118	31.52
104	3	0.118	33.52
105	3	0.118	35.72
106	3	0.118	37.52
107	3	0.118	39.72
108	3	0.118	42.52
109	3	0.110	43.72
110	3	0.110	45.92
111	3	0.110	48.72
112	3	0.110	51.32
113	4	0.186	34.72
114	4	0.186	35.32
115	4	0.176	36.72
116	4	0.186	39.92
117	4	0.186	41.52
118	4	0.186	43.52
119	4	0.186	46.92
120	4	0.186	47.92
121	4	0.186	51.32
122	5	0.285	37.52
123	5	0.274	39.72
124	5	0.274	41.72
125	5	0.285	43.32
126	5	0.274	46.12
127	5	0.270	47.12
128	5	0.265	51.12
129	5	0.265	51.92
130	6	0.392	40.92
131	6	0.383	43.32
132	6	0.374	45.12
133	6	0.374	48.32
134	6	0.374	51.12
135	6	0.363	52.32
136	6	0.363	54.72
137	7	0.529	44.92
138	7	0.519	47.32
139	7	0.500	49.12
140	7	0.500	51.92
141	7	0.491	54.52
142	8	0.697	50.32
143	8	0.687	51.32
144	8	0.678	52.32
145	8	0.678	53.32
146	8	0.668	53.72
147	8	0.638	58.32

CHAPTER VI

CORRELATING THE DATA

After collecting the data the task of correlating the data was begun. A plot of the data on Nesbit's (10) chart is shown in Fig. 9. His chart shows the combinations of the Reynolds number for the gas and liquid which will produce the various flow patterns. As can be seen all of the data taken falls within the region of complete mist as defined by Nesbit.

A comparison of the data obtained, to the pressure drop as predicted by Martinelli shows that his correlations are not applicable to the data gathered in this test. Pressure drops as low as 1.1 times the pressure drop for the gas flowing alone were encountered. Indeed, it would seem that as the liquid rate was gradually increased from zero that the pressure drop should also gradually increase from that due to the gas alone.

Thus Martinelli's correlation has been disregarded as it does not seem applicable to the case of mist flow.

In order to determine the validity of the Yagi and Sasaki equation (Eq. 7), it was used to calculate the pressure drop of each of the runs. In order to use their equation some assumption as to the value of the average liquid velocity had to be made. The velocity of the liquid was assumed to be the same as that of the gas. With this assumption, Eq. 7 gives pressure drops for mist flow approximately eighteen times the actual pressure drops

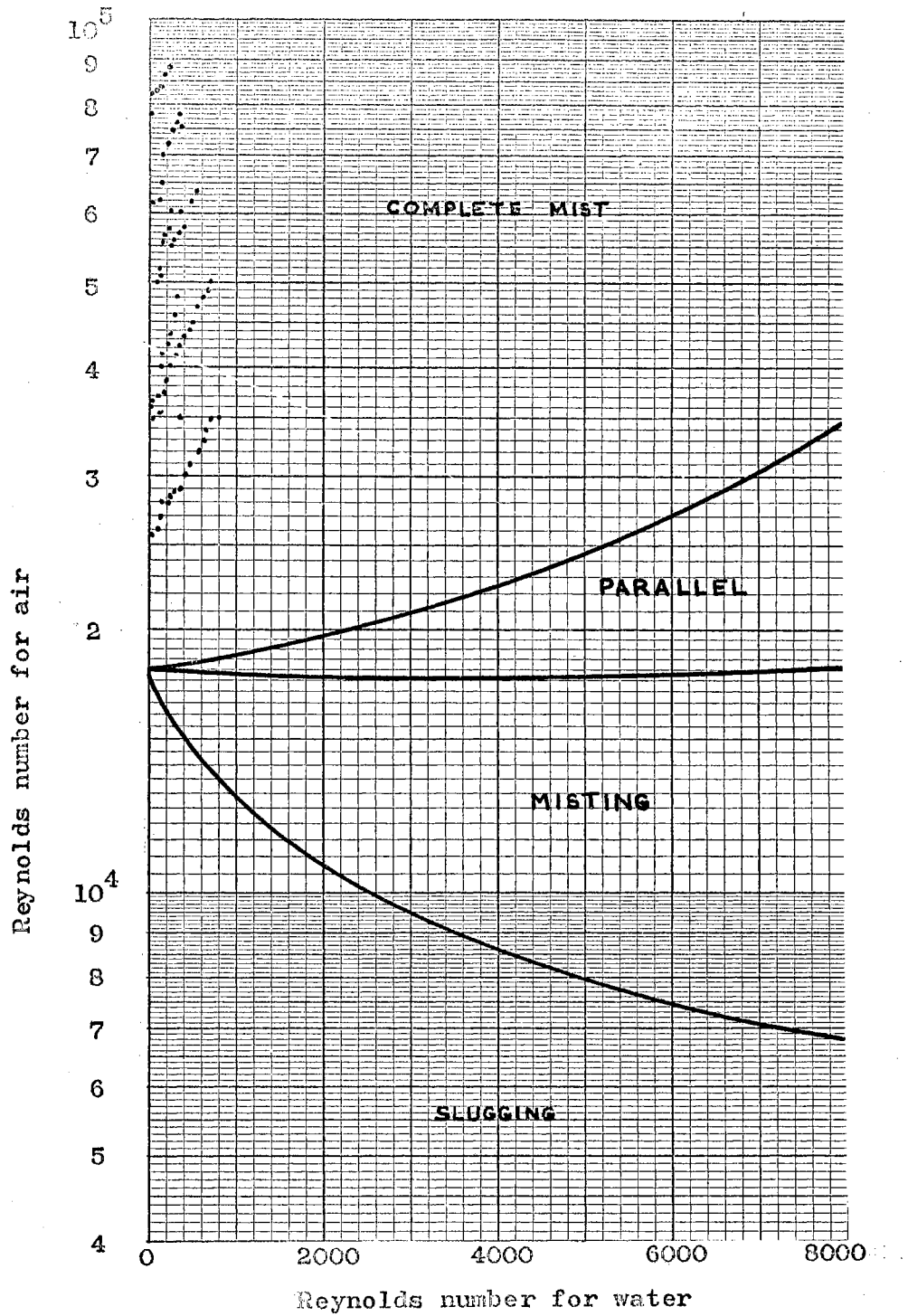


Fig. 9. Nesbit's flow pattern chart

measured. It is felt that the Yagi and Sasaki equation would not be useful as a practical tool to predict pressure drop in mist flow. Usually some special method would be required to obtain the actual liquid velocity in mist flow.

The procedure used to correlate the data collected in this test, consisted of listing the factors that could affect the pressure drop and arrange them into dimensionless groups. This is similar to the procedure that Martinelli used. The dimensionless numbers used as the factors which were thought to affect pressure drop were Re_g , W_l/W_g , ρ_l/ρ_g , and μ_l/μ_g .

The pressure drop of the mixture was computed as a function of the air flowing alone at the same average static pressure as that of the mixture. Therefore:

$$\left[\frac{\Delta P}{\Delta L} \right]_{\text{mist}} = \phi_{\text{mist}} \left[\frac{\Delta P}{\Delta L} \right]_g \quad (9)$$

where $\left[\frac{\Delta P}{\Delta L} \right]_{\text{mist}}$ = pressure drop for mist flow, psi per ft;

$\left[\frac{\Delta P}{\Delta L} \right]_g$ = pressure drop for gas flowing alone, psi per ft;
and

ϕ_{mist} = a dimensionless parameter.

The dimensionless parameter, ϕ_{mist} , was then said to be a function of the parameter, X_{mist} . X_{mist} was defined as:

$$X_{\text{mist}} = Re_g \frac{W_l}{W_g} \frac{\rho_l}{\rho_g} \frac{\mu_l}{\mu_g} \quad (10)$$

where the symbols are as used before.

The values of ϕ_{mist} and X_{mist} were calculated by using Eq. 9 and 10.

A plot of ϕ_{mist} versus X_{mist} is shown in Fig. 10. This

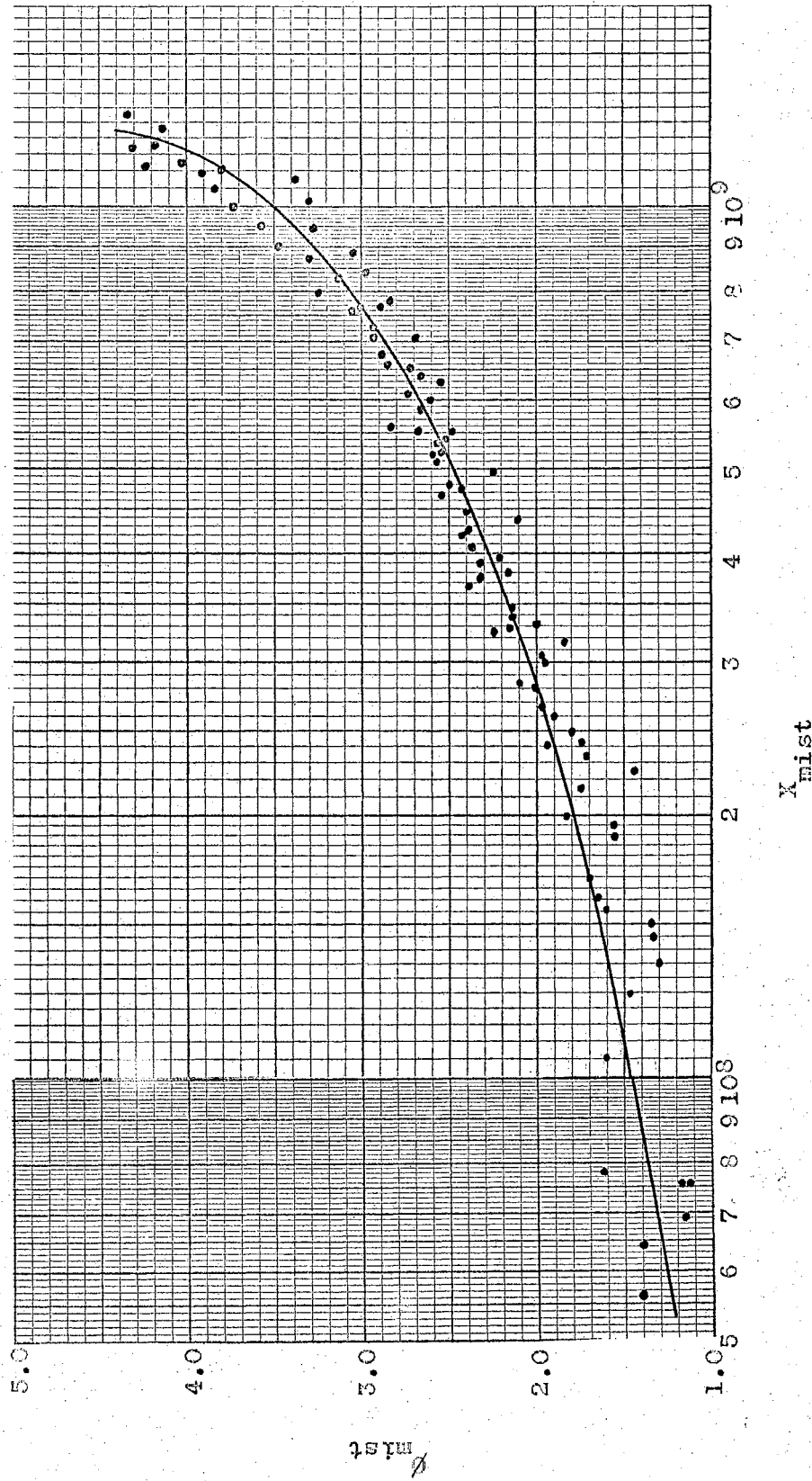


Fig. 10. Relation of ϕ_{mist} to X_{mist}

plot could serve as the relation between ϕ_{mist} and X_{mist} , however, it is thought that a mathematical expression of $\phi_{\text{mist}} = f(X_{\text{mist}})$ would be a much more useful tool. Therefore, by trial and correction methods, exponents of ϕ_{mist} and X_{mist} were determined such that ϕ_{mist} versus X_{mist} would plot into a straight line on a linear scale as shown in Fig. 11. From Fig. 11 an equation could be determined of the form:

$$\phi_{\text{mist}}^n = m X_{\text{mist}}^p + b \quad (11)$$

where n, m, p, and b are constants to be determined and the other symbols are as previously explained.

The values of n, m, p, and b that were found to give the best results were:

$$n = 0.293$$

$$m = 0.00436$$

$$p = 0.257$$

$$b = 0.562.$$

Thus the final form of Eq. 11 becomes:

$$\phi_{\text{mist}}^{0.293} = (0.00436)X_{\text{mist}}^{0.257} + 0.562. \quad (12)$$

As an example of how to predict pressure drop for mist flow using Eq. 9, 10, and 12, assume the data of run no. 66:

Air rate = 6 cfm,

Water rate = 0.286 lbs per min,

Average static pressure = 54.78 in. hg abs,

Pressure drop for gas flowing alone = 0.360 psi per ft,

Temperature = 65° F,

Diameter = 0.0251 ft, and

Area = 4.94×10^{-4} sq ft.

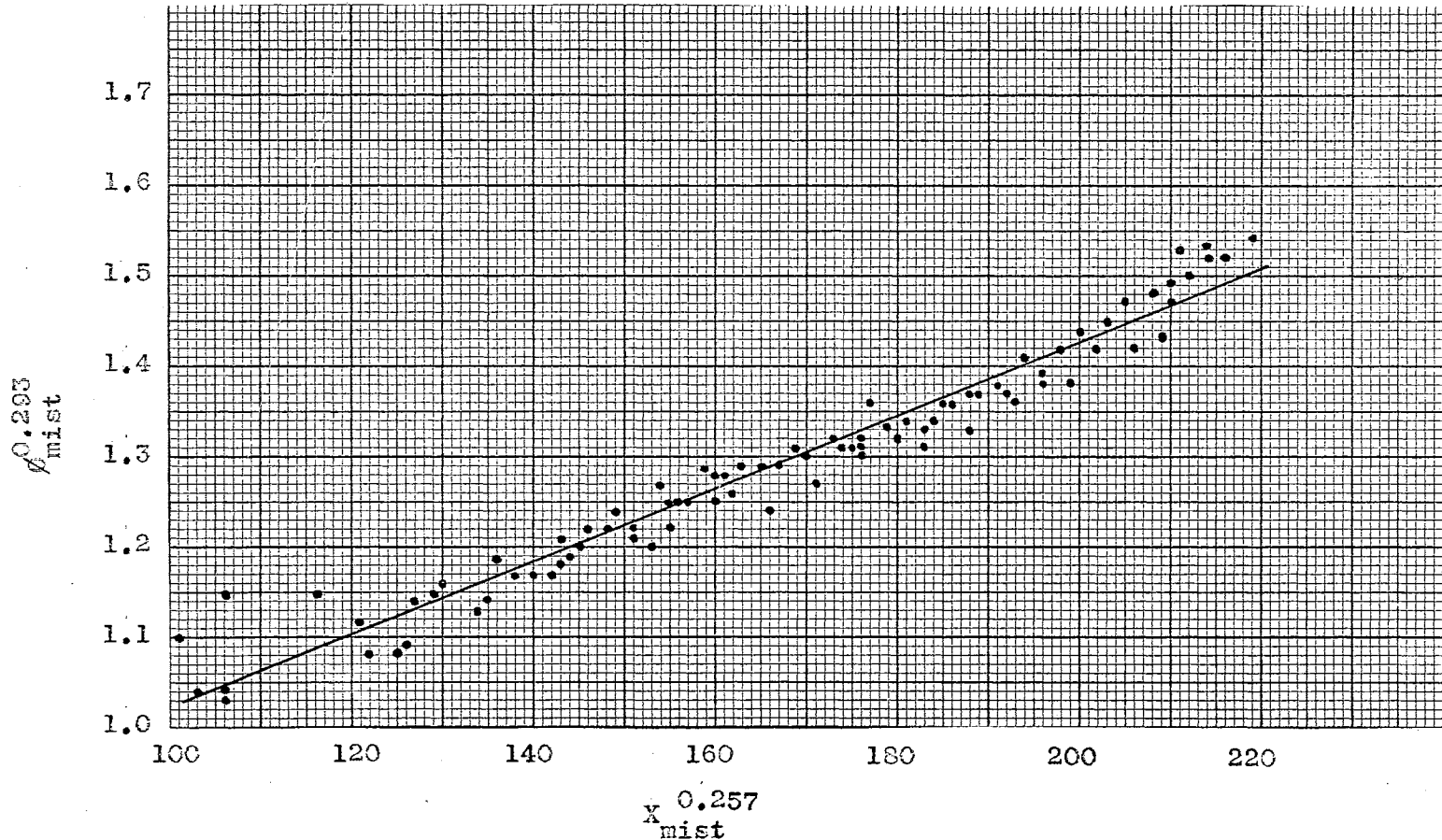


Fig. 11. Relation between $\phi_{mist}^{0.293}$ and $X_{mist}^{0.257}$

Solution:

$$54.78 \text{ in. hg abs} = 3880 \text{ lbs per sq ft abs}$$

$$\rho_g = \frac{P}{RT} \quad (13)$$

where P = pressure of gas, lbs per sq ft;

R = gas constant, ft per °R; and

T = absolute temperature, °R.

$$65^\circ \text{ F} = 525^\circ \text{ R}$$

$$\rho_g = \frac{3880}{53.3 \times 525} = 0.1382 \text{ lbs per cu ft} \quad \text{Eq. 13}$$

$$\rho_1 = 62.4 \text{ lbs per cu ft}$$

$$\frac{\rho_1}{\rho_g} = \frac{62.4}{0.1382} = 451$$

$$W_g = \rho_g \times V_g \quad (14)$$

where V_g and ρ_g are as used previously.

$$W_g = 0.1382 \times 6 = 0.830 \text{ lbs per min} \quad \text{Eq. 14}$$

$$\frac{W_1}{W_g} = \frac{0.286}{0.830} = 0.345$$

$$\mu_1 = 7.53 \times 10^{-4} \text{ lbs per sec-ft}$$

$$\mu_g = 1.239 \times 10^{-5} \text{ lbs per sec-ft}$$

$$\frac{\mu_1}{\mu_g} = \frac{7.53 \times 10^{-4}}{1.239 \times 10^{-5}} = 60.8$$

$$\text{Velocity} = \frac{V_g}{A} \quad (15)$$

where A = cross-section of flow channel, sq ft; and V_g is as used before.

$$\text{Velocity} = \frac{6}{60 \times 4.94 \times 10^{-4}} = 202.2 \text{ ft per sec Eq. 15}$$

$$\text{Re}_g = \frac{\rho_g U_g d}{\mu_g} \quad (16)$$

where the symbols are as used before.

$$Re_g = \frac{0.1382 \times 202.2 \times 0.0251}{1.239 \times 10^{-5}} = 56,740 \quad \text{Eq. 16}$$

$$X_{mist} = 56,740 \times 451 \times 0.345 \times 60.8 = 5.359 \times 10^8 \quad \text{Eq. 10}$$

$$X_{mist}^{0.257} = 175.1$$

$$\phi_{mist}^{0.293} = 0.00436 \times 175.1 + 0.562 \quad \text{Eq. 12}$$

$$= 1.325$$

$$\phi_{mist} = 2.61$$

$$\left[\frac{\Delta P}{\Delta L} \right]_{mist} = 2.61 \times 0.360 = 0.941 \text{ psi per ft} \quad \text{Eq. 9}$$

The measured pressure drop was 0.924 psi per ft. Therefore, the error is:

$$\frac{0.941 - 0.924}{0.924} = 1.8 \text{ percent.}$$

These computations are a sample of those which were made for each set of data. The results for all of the runs are listed in Table III.

The average error was found to be 5.9 percent.

TABLE III
CORRELATION ERROR

Run No.	Pressure drop, measured; psi per ft	Pressure drop, computed; psi per ft	Error; percent
1	0.314	0.281	-10.2
2	0.334	0.334	0.1
3	0.402	0.382	- 4.9
4	0.441	0.420	- 4.6
5	0.451	0.456	1.2
6	0.460	0.490	6.5
7	0.470	0.526	11.9
8	0.500	0.556	11.3
9	0.540	0.581	7.6
11	0.530	0.586	10.6
12	0.550	0.609	10.9
13	0.564	0.628	11.4
14	0.608	0.649	6.8
15	0.608	0.675	11.0
16	0.628	0.695	10.7
17	0.705	0.703	- 0.1
18	0.745	0.718	- 3.5
19	0.774	0.731	- 5.4
20	0.765	0.750	- 1.8
21	0.804	0.767	- 4.5
23	0.774	0.784	1.4
24	0.795	0.815	2.5
25	0.804	0.842	4.7
26	0.833	0.868	4.2
27	0.882	0.893	1.2
28	0.924	0.906	- 1.9
29	0.944	0.924	- 1.9
30	0.982	0.942	- 4.0
31	1.000	0.963	- 3.6
32	1.010	0.980	- 2.9
33	1.090	0.982	- 9.9
34	1.100	1.001	- 8.9
36	0.460	0.310	-32.5
37	0.440	0.409	- 6.9
38	0.480	0.489	1.8
39	0.510	0.556	9.1
40	0.598	0.605	1.1
41	0.579	0.745	11.5
42	0.619	0.684	10.5
43	0.688	0.715	4.0
44	0.707	0.748	5.8
45	0.735	0.780	6.2
47	0.314	0.301	- 3.9
48	0.372	0.394	6.0
49	0.402	0.476	18.4

TABLE III (Continued)

Run No.	Pressure drop, measured; psi per ft	Pressure drop, computed; psi per ft	Error percent
50	0.549	0.519	- 5.3
51	0.588	0.565	- 3.8
52	0.600	0.610	1.7
53	0.648	0.645	- 0.4
54	0.688	0.678	- 1.3
55	0.707	0.704	- 0.4
56	0.725	0.740	2.1
58	0.450	0.417	- 7.2
59	0.510	0.543	6.4
60	0.688	0.614	-10.6
61	0.735	0.691	- 5.8
62	0.745	0.767	2.9
63	0.874	0.791	- 9.4
64	0.882	0.844	- 4.2
65	0.904	0.897	- 0.7
66	0.924	0.941	1.8
67	1.020	0.954	- 6.4
68	0.963	0.983	2.1
70	0.963	1.029	6.8
71	1.030	1.046	1.5
72	1.040	1.085	4.3
73	1.080	1.100	1.8
74	1.140	1.122	- 1.5
76	0.431	0.392	- 8.8
77	0.491	0.513	4.5
78	0.579	0.596	2.9
79	0.707	0.649	- 8.1
80	0.707	0.710	0.5
81	0.774	0.760	- 1.7
82	0.833	0.795	- 4.5
84	0.717	0.515	-28.0
85	0.755	0.675	-10.5
86	0.748	0.800	2.1
87	0.874	0.878	0.5
88	1.000	0.911	- 8.8
89	1.060	0.957	- 9.6
90	1.090	1.026	- 5.8
91	1.120	1.067	- 4.6
92	1.160	1.116	- 3.7
93	1.170	1.155	- 1.2
95	1.170	1.187	1.4
97	0.924	0.636	-31.1
98	1.030	0.789	-23.3
99	1.050	0.945	- 9.9
100	1.090	1.047	- 3.9
101	1.150	1.110	- 3.4
102	1.180	1.186	0.5

CHAPTER VII

COMPUTATIONS

All computations were made with an IBM 650 digital computer. The values of the pressure drop for each run were computed using Eq. 9, 10, and 12 as previously mentioned. The pressure drop was also computed using the Yagi and Sasaki equation (Eq. 7). The values of ϕ_{mist} and X_{mist} were computed using Eq. 9 and 10 and using the actual pressure drop. From these values $\phi_{\text{mist}}^{0.293}$ and $X_{\text{mist}}^{0.257}$ were calculated. A sample of the calculation of $\phi_{\text{mist}}^{0.293}$ and $X_{\text{mist}}^{0.257}$ as carried out for each run is now shown in detail. Again assume the data of run no. 66:

Air rate = 6 cfm,

Water rate = 0.286 lbs per min,

Average static pressure = 54.78 in. hg abs,

Pressure drop of mixture = 0.924 psi per ft,

Pressure drop of the gas flowing alone = 0.360 psi
per ft,

Temperature = 65° F,

Diameter = 0.0251 ft, and

Area = 4.94×10^{-4} sq ft.

Calculations:

54.78 in. hg abs = 3880 lbs per sq ft abs

65° F = 525° R

$$\rho_g = \frac{3880}{53.3 \times 525} = 0.1382 \text{ lbs per cu ft} \quad \text{Eq. 13}$$

$$\rho_l = 62.4 \text{ lbs per cu ft}$$

$$\frac{\rho_l}{\rho_g} = \frac{62.4}{0.1382} = 451$$

$$W_g = 0.1382 \times 6 = 0.830 \text{ lbs per min} \quad \text{Eq. 14}$$

$$\frac{W_l}{W_g} = \frac{0.286}{0.830} = 0.345$$

$$\mu_l = 7.53 \times 10^{-4} \text{ lbs per sec-ft}$$

$$\mu_g = 1.239 \times 10^{-5} \text{ lbs per sec-ft}$$

$$\frac{\mu_l}{\mu_g} = \frac{7.53 \times 10^{-4}}{1.239 \times 10^{-5}} = 60.8$$

$$\text{Velocity} = \frac{6}{60 \times 4.94 \times 10^{-4}} = 202.2 \text{ ft per sec} \quad \text{Eq. 15}$$

$$Re_g = \frac{0.1382 \times 202.2 \times 0.0251}{1.239 \times 10^{-5}} = 56,740 \quad \text{Eq. 16}$$

$$X_{\text{mist}} = 56,740 \times 451 \times 0.345 \times 60.8 = 5.359 \times 10^8 \quad \text{Eq. 10}$$

$$X_{\text{mist}}^{0.257} = 175.1$$

$$\phi_{\text{mist}} = \frac{0.924}{0.360} = 2.56 \quad \text{Eq. 9}$$

$$\phi_{\text{mist}}^{0.293} = 1.318$$

The values of ϕ_{mist} , X_{mist} , $\phi_{\text{mist}}^{0.293}$, and $X_{\text{mist}}^{0.257}$ were plotted as explained before. All of the calculated values of these four parameters are tabulated in Table IV.

TABLE VI
CORRELATION PARAMETERS

Run No.	X_{mist}	ϕ_{mist}	$X_{mist}^{0.257}$	$\phi_{mist}^{0.293}$
1	1,709 $\times 10^8$	1,697	130,5	1,167
2	2,499	1,805	143,9	1,188
3	3,316	2,172	154,8	1,255
4	4,043	2,383	162,9	1,289
5	4,777	2,437	170,0	1,298
6	5,503	2,486	176,3	1,305
7	6,325	2,540	182,7	1,314
8	7,053	2,702	187,9	1,338
9	7,658	2,918	191,9	1,368
11	7,792	2,964	192,8	1,361
12	8,391	2,972	196,5	1,376
13	8,887	3,048	199,4	1,386
14	9,443	3,286	202,5	1,417
15	10,142	3,286	206,3	1,417
16	10,716	3,394	209,2	1,430
17	10,958	3,810	210,4	1,479
18	11,384	4,027	212,5	1,504
19	11,774	4,183	214,4	1,520
20	12,336	4,135	216,9	1,515
21	12,838	4,345	219,2	1,538
23	6,595	2,866	184,7	1,361
24	7,095	2,944	188,2	1,372
25	7,664	3,000	192,0	1,379
26	8,233	3,131	195,5	1,397
27	8,682	3,315	198,2	1,420
28	8,985	3,486	200,0	1,441
29	9,481	3,589	202,7	1,454
30	9,953	3,762	205,3	1,474
31	10,431	3,846	207,8	1,483
32	10,938	3,914	210,3	1,491
33	11,126	4,257	211,3	1,528
34	11,626	4,313	213,7	1,534
36	0,779	1,625	106,7	1,152
37	1,559	1,571	127,5	1,141
38	2,354	1,726	141,7	1,173
39	3,157	1,847	152,8	1,197
40	3,783	2,174	160,1	1,255
41	4,352	2,113	166,0	1,245
42	4,930	2,267	171,4	1,271
43	5,430	2,529	175,7	1,312
44	5,965	2,608	180,0	1,324
45	6,527	2,722	184,2	1,341
47	0,759	1,129	106,0	1,036
48	1,491	1,352	126,0	1,092
49	2,274	1,461	140,5	1,117
50	2,790	2,010	148,0	1,227
51	3,387 $\times 10^8$	2,169	155,6	1,254

TABLE VI (Continued)

Run No.	X _{mist}	Ø _{mist}	X ^{0.257} _{mist}	Ø ^{0.293} _{mist}
52	3.973 x 10 ⁸	2,214	162.1	1.262
53	4.476	2,400	167.2	1.292
54	5.104	2,586	172.9	1.321
55	5.530	2,667	176.5	1.333
56	6.103	2,735	181.0	1.342
58	0.757	1,168	105.9	1.046
59	1.460	1,335	125.3	1.088
60	2.015	1,834	136.2	1.194
61	2.671	1,981	146.4	1.221
62	3.325	2,008	154.9	1.226
63	3.667	2,394	158.8	1.291
64	4.218	2,423	164.6	1.296
65	4.794	2,490	170.1	1.306
66	5.359	2,566	175.1	1.318
67	5.629	2,865	177.3	1.361
69	5.840	2,675	179.0	1.334
70	6.386	2,675	183.2	1.334
71	6.737	2,893	185.7	1.365
72	7.272	2,929	189.4	1.370
73	7.584	3,068	191.4	1.388
74	7.962	3,257	193.8	1.413
76	0.690	1,146	103.4	1.040
77	1.346	1,312	122.7	1.083
78	1.939	1,564	134.8	1.140
79	2.429	1,942	142.9	1.214
80	2.981	1,953	150.6	1.216
81	3.477	2,150	156.7	1.251
82	3.879	2,333	161.1	1.281
84	0.641	1,411	101.5	1.106
85	1.253	1,489	120.5	1.123
86	1.897	1,561	134.1	1.139
87	2.434	1,776	142.9	1.183
88	2.842	2,105	148.7	1.243
89	3.251	2,264	154.0	1.270
90	3.757	2,329	159.8	1.281
91	4.220	2,434	164.7	1.297
92	4.661	2,532	168.9	1.312
93	5.150	2,594	173.3	1.322
95	5.223	2,543	173.9	1.314
97	0.564	1,404	98.2	1.104
98	1.064	1,622	115.6	1.152
99	1.625	1,653	128.8	1.158
100	2.154	1,758	138.5	1.179
101	2.607	1,910	145.5	1.208
102	3.048 x 10 ⁸	1,973	151.4	1.220

CHAPTER VIII

CONCLUSIONS

Much work has been done by many investigators toward deriving an expression of the pressure drop of two-component, two-phase flow. Martinelli and others have expressed the pressure drop for two-component, two-phase flow in terms of the Reynolds number of each component in the flow.

Much evidence has been accumulated which points toward the idea that a correlation for predicting the pressure drop for each type of flow pattern would be much more accurate.

The data gathered in this test indicated that Martinelli's correlation does not apply to mist flow. The Yagi and Sasaki relation seemed plausible, however, the difficulty in evaluating the average liquid velocity makes this equation unwieldy.

In this experiment it was found that the pressure drop which occurs during vertically upward, isothermal, mist flow can be predicted by the use of:

$$\left[\frac{\Delta P}{\Delta L} \right]_{\text{mist}} = \phi_{\text{mist}} \left[\frac{\Delta P}{\Delta L} \right]_g, \quad (9)$$

$$\phi_{\text{mist}}^{0.293} = (0.00436) X_{\text{mist}}^{0.257} + 0.562, \quad (12)$$

$$\text{and } X_{\text{mist}} = \text{Re}_g \frac{W_1}{W_g} \frac{\rho_1}{\rho_g} \frac{\mu_1}{\mu_g}, \quad (10)$$

where $\left[\frac{\Delta P}{\Delta L} \right]_g$ = pressure drop for gas flowing alone, psi per ft;

Re_g = Reynolds number of gas flowing alone;

W_l = Liquid rate, lbs per min;

W_g = gas rate, lbs per min;

ρ_l = liquid density, lbs per cu ft;

ρ_g = gas density, lbs per cu ft;

μ_l = liquid viscosity, lbs per sec-ft; and

μ_g = gas viscosity, lbs per sec-ft.

The range of values used were:

Air rate, 0.376 to 1.29 lbs per min;

Water rate, 0 to 0.667 lbs per min;

Re_g , 25,700 to 88,300.

It was noted that at air rates smaller than 4 cfm it was impossible to maintain mist flow in the test section. The water tended to cling to the entire periphery of the wall of the test section or proceed up the tube in streams against the wall depending on the water rate. Visual observation was used to insure that the data being taken was of mist flow. Reproducibility was remarkably good. Time after time the same pressure drop was noted at the same air and water rate.

The correlations derived from this experiment (Eq. 9, 10, and 12) will predict the pressure drop of vertically upward, mist flow of air and water within five percent of the actual value.

BIBLIOGRAPHY

1. Bergelin, O. P., "Flow of Gas-Liquid Mixtures," Chem. Engr., vol. 56, May 1949, pp 104-106.
2. Bergelin, O. P., P. K. Kegel, F. G. Carpenter, and Carl Gazley, Jr., "Cocurrent Gas-Liquid Flow in Vertical Tubes," Heat Transfer and Fluid Mechanics Institute, Berkeley, California, 19-28 (1949). Also A.S.M.E., May 1949.
3. Boelter, L. M. K. and R. H. Kepner, "Pressure Drop Accompanying Two-Component Flow Through Pipes," Ind. and Engr. Chem., vol. 31, 1939, pp 426-434.
4. Gazley, Carl Jr., and O. P. Bergelin, "Discussion of Proposed Correlation of Data for Two-Phase, Two-Component Flow in Pipes," Chem. Eng. Progress, vol. 45, 1949, pp 45-48
5. Gosline, J. E., "Experiments on the Vertical Flow of Gas-Liquid Mixtures in Glass Pipes," Trans. A.I.M.E. (Pet. Dev. and Tech.), 118, 56 (1936).
6. Johnson, H. A. and A. H. Abou-Sabe, "Heat Transfer and Pressure Drop for Turbulent Flow of Air-Water Mixtures in a Horizontal Pipe," A.S.M.E. Trans., vol. 74, no. 6, August 1952, pp 977-984.
7. Lockhart, R. W. and R. C. Martinelli, "Proposed Correlation of Data for Isothermal Two-Phase, Two-Component Flow in Pipes," Chem. Engr. Progress, vol. 45, no. 1, January 1949.
8. Martinelli, R. C. and L. M. K. Boelter, "Isothermal Pressure Drop for Two-Phase, Two-Component Flow in a Horizontal Pipe," Trans. A.S.M.E., February 1944, pp 139-151.
9. Martinelli, R. C., J. A. Putnam, and R. W. Lockhart, "Two-Phase, Two-Component Flow in the Viscous Region," Trans. Amer. Inst. of Chem. Engineers, vol. 42, no. 4, August 1946, p 681.
10. Nesbit, J. R., "Characteristics of Two-Phase Fluid Flow," Carnegie Institute of Technology, B. S. Thesis, January 1940, p 21.

11. Taylor, T. H. M., "Pressure Drop Accompanying Isothermal, Two-Component, Two-Phase Flow in a Horizontal Glass Pipe," M. S. Thesis, University of California, 1942.
12. Thomsen, E. G., "Pressure Drop Accompanying Two-Component Flow in a Closed Conduit with Various Liquids and Air," M. S. Thesis, University of California, 1941.
13. Yagi, Sakae and Yasuo Kato, "Fundamental Studies of Horizontal-Pipe Reactor," Chemical Engr. (Japan) 15, 1951, pp 317-322.
14. Yagi, Sakae and T. Sasaki, "Vertical Pipe Reactor II, Pressure Drop in Gas-Liquid, Two-Phase Flow," Chem. Engineering (Japan) 17, 1953, pp 216-223.

APPENDIX

LIST OF EQUIPMENT

- 1 - Fischer and Porter rotameter #B-851349, 0-8.5 cfm air at 0 psig and 100° F, tube #5A-25, 3/8 in. pipe inlet and outlet.
- 1 - Fischer and Porter flowrator #J5-1812, 45-132 lbs per hr of liquid of specific gravity of 0.78-0.81.
- 1 - Fischer and Porter flowrator #J5-1811, tube #2K-25, 19-69 lbs per hr of liquid of specific gravity of 0.78-0.81.
- 2 - Meriam Instrument Co. 36 in. standard cleanout manometers using mercury.
- 1 - Commercial Filters Corp. fulflow filter, Model WF6, 2 in. pipe inlet and outlet, cotton batting packing.
- 1 - Fisher Governor Co. pressure regulator, type 630, serial no. 2035007; maximum inlet pressure, 1000 psi; maximum outlet pressure, 30 psi.
- 1 - Fairbanks-Morse Co. centrifugal pump, 1750 rpm, fig. 5500, no. 2969.

The air was supplied by a Pennsylvania Pump and Compressor Co. 2 stage air compressor, serial no. 4727, class 11AT, rated at 100 cfm at 400 rpm. The compressor was driven by a 25 hp electric motor.

Miscellaneous valving and piping to properly connect the above equipment.

VITA

William Dean Leonard

Candidate for the Degree of
Master of Science

Thesis: PRESSURE DROP OF MIST FLOW OF AIR AND WATER IN A
VERTICAL PIPE

Major Field: Mechanical Engineering

Biographical:

Personal data: Born at Stillwater, Oklahoma, November 29,
1934, the son of Carroll M. and Helen C. Leonard.

Education: Attended grade school in Stillwater, Oklahoma;
graduated from Stillwater High School in 1953;
received the Bachelor of Science degree from Oklahoma
State University, with a major in mechanical engineer-
ing, in May 1957; completed the requirements for the
Master of Science degree in August, 1958.

Experience: Owned and operated a hobby shop successfully
for eight years during highschool and college career;
employed as a Junior Engineer at Boeing Airplane
Company, Wichita, Kansas, during summer of 1957;
Engineer-in-Training, no. 480, Oklahoma.

Professional organization: American Society of Mechanical
Engineers.

Honorary organizations: Pi Tau Sigma, 1955; Phi Kappa Phi,
1957.

Honors and awards: Pan American graduate fellowship, 1957-
1958; second-place in American Society of Mechanical
Engineers' regional papers contest, 1957.